

THE STRUCTURE OF THE WELDED ZONE AND PHASE TRANSFORMATION BEHAVIOR OF NI-BASED BULK GLASS FORMING ALLOY

D. V. Louzguine-Luzgin^{1,*}, G. Xie¹, T. Tsumura², K. Nakata², Y. Murakami¹, H. M. Kimura¹ and A. Inoue¹

¹*Institute for Materials Research, Tohoku University, Katahira 2-1-1, Aoba-Ku, Sendai 980-8577, Japan*

²*Joining & Welding Research Institute, Osaka University, Mihogaoka, Ibaraki, Osaka 567-0047, Japan*

ABSTRACT

The crystallization behavior and the structure of the welded samples of the $\text{Ni}_{53}\text{Nb}_{20}\text{Ti}_{10}\text{Zr}_8\text{Co}_6\text{Cu}_3$ glassy alloy are studied. A large supercooled liquid region of about 50 K observed enables its successful welding. On heating the supercooled liquid crystallizes by polymorphous mechanism forming a single metastable hR14 Ni_4Ti_3 phase which further transforms at higher temperature forming several equilibrium phases. Its composition was found to be very close (equal within the confidential interval) to that of the glassy phase. The kinetic analysis confirmed the interface-controlled polymorphous transformation mechanism observed.

Good bonding between two glassy samples was obtained after welding. The results indicate that with an increase in the welding speed from 2 to 3 m/min the structure of the welded zone changes from the amorphous + hR14 Ni_4Ti_3 crystalline phase to an almost single amorphous one. By adjusting the welding speed one can obtain the desired microstructure. The samples electron-beam welded at the beam current of 4 mA and voltage of 60 kV at a speed of 4 m/min were found to be almost amorphous. The results indicate successful welding of the Ni-based glassy samples.

INTRODUCTION

Bulk glassy alloys with a size exceeding 1 mm in three dimensional space were obtained by stabilization of the supercooled liquid against crystallization at the relatively low cooling rate of less than 100 K/s from liquid state in the various, mostly multi-component, metallic alloys.¹⁻³ These alloys are promising materials for structural applications as they exhibit high mechanical strength, high hardness, good fracture toughness, good corrosion resistance², etc.

In particular, bulk glass formation was achieved in various Ni-based alloy systems: Ni-Zr-Ti (Si,Sn)^{4,5}, Ni-Nb-Ti-Zr⁶, Ni-Nb-Ti⁷, Ni-Nb-Ti-Hf^{8,9}, Ni-Nb-Sn¹⁰ and so on, which are actually a group of LTM-ETM or LTM-ETM-M alloys (where LTM is(are) late transition metal(s), ETM is(are) early transition metal(s) and M is metalloïd or Sn). These alloys are promising candidates for structural applications owing to their high strength attaining 3 GPa. $\text{Ni}_{53}\text{Nb}_{20}\text{Ti}_{10}\text{Zr}_8\text{Co}_6\text{Cu}_3$ bulk glassy alloy exhibits a high tensile fracture strength of 2700 MPa and a critical diameter of 3 mm¹¹. $\text{Ni}_{50}\text{Zr}_{10}\text{Ti}_{15}\text{Si}_3\text{Sn}_2\text{Nb}_7$ bulk glassy alloy which showed a significant plastic deformation of 6.5 % to failure¹² may contain nanoparticles which are not detectable by an X-ray diffraction (XRD) technique. Devitrification behavior of Ni-Nb-Ti¹³, Ni-Nb-Ti-Zr, Ni-Nb-Ti-Zr and Ni-Nb-Ti-Zr-Pt¹⁴ glassy alloys has been studied recently.

* Corresponding author. Tel: +081(22)215-2592, Fax: +081(22)215-2381, e-mail: dml@imr.tohoku.ac.jp

At the same time a limited size of bulk metallic glassy samples requires bonding technology to obtain industrial-size samples. In the present work we study the crystallization and welding behavior of the $Ni_{53}Nb_{20}Ti_{10}Zr_3Co_6Cu_3$ glassy alloy. This alloy is a good candidate for study as it has one of the highest GFAs among Ni-based alloys and a large supercooled liquid region.

EXPERIMENTAL PROCEDURE

An ingot of the $Ni_{53}Nb_{20}Ti_{10}Zr_3Co_6Cu_3$ alloy was prepared by arc-melting using pure elements of 99.9 mass% purities in an argon atmosphere. Ni-based metallic glassy ribbon with a width of 40 mm and thickness of 25 μm used in this study was produced by rapid solidification of the melt on a single copper roller at a roller tangential velocity of 42 m/s. The structure of the samples was examined by X-ray diffractometry (XRD) with monochromatic CuK_{α} radiation. The structure of the welded bead was studied using a micro-area XRD (CuK_{α} radiation) with a collimator size of 30 μm . The phase transformations were studied by differential scanning calorimetry (DSC) at a heating rate of 0.67 K/s and differential isothermal calorimetry (DIC).

As the laser welding heat source, diode laser welding apparatus KATAOKA LD-YAG HP300a was used. The welding was carried out at the diameter of the laser beam of 0.3 mm, the laser beam power of 26 W, and the welding speed range of 2 to 3 m/min. MITSUBISHI EM-9HIB election beam welding apparatus was used as the election welding heat source. The welding was carried out at the accelerating voltage of 60 kV, beam current range of 3 to 5 mA, welding speed of 4 m/min under an evacuated atmosphere of about 0.1 Pa. In order to prevent crystallization at the heat affected zone copper plates were used as the cover and backing plates. The cover plate has had a slit of 0.6 mm in width which is similar in size to the laser/electron spot diameter.

Transmission electron microscopy (TEM) investigation was carried out using a JEM 2010 (JEOL) microscope operating at 200 kV equipped with an energy dispersive X-ray (EDX) spectrometer of 0.1 keV resolution. The samples for TEM were prepared by the ion-polishing technique.

RESULTS

Thermal stability and crystallization behavior of the glassy alloy.

First of all the crystallization behaviour of the $Ni_{53}Nb_{20}Ti_{10}Zr_3Co_6Cu_3$ alloy on heating was studied in order to determine the temperature interval of welding. A DSC trace taken within the present work is shown in Fig. 1 (a). The sample undergoes glass transition, followed by a large supercooled liquid region and then two exothermic reactions due to crystallization. The glass transition temperature (T_g), temperature of crystallization (T_c), and melting temperature (T_m) are 845 K, 897 K, and 1265 K, respectively. This alloy has a very high T_{ig} of 0.67.

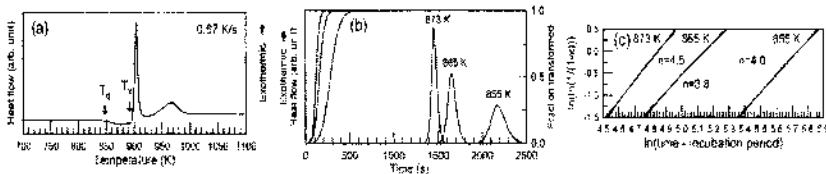


Figure 1. (a) DSC trace and (b) DIC traces obtained at 855, 865 and 873 K for the studied alloy. Fraction transformed in (b) is shown without incubation period. (c) Avrami analysis for the fraction transformed as a function of time.

Upon heating the studied glassy alloy initially devitrifies through a supercooled liquid producing a multicomponent hR14 Ni₄Ti₃ phase (the lattice parameters a=1.12nm, c=0.51 nm) starting at about 900 K and hR14 Ni₆Nb₆ phase at about 950 K (Fig. 2).

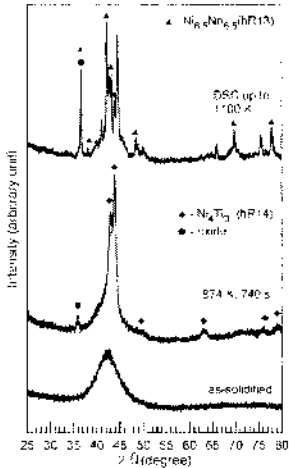


Figure 2. XRD patterns of the studied alloy in as-solidified and annealed states as indicated.

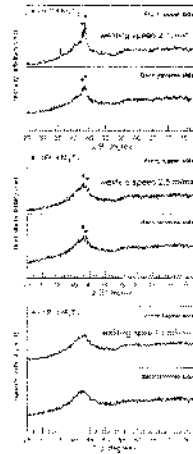


Figure 3. Micro-area XRD patterns of the laser-beam welded samples. Welded bead, upper and bottom side.

The isothermal calorimetry traces obtained at different temperatures shown in Fig. 1 (b) were analyzed using an Avrami method (including the least squares fitting of the Avrami plot) for the fraction transformed as a function of time (Fig. 1 (c)) according to the following kinetic law¹⁵ for the volume fraction (x) transformed as a function of time (t):

$$x(t) = 1 - \exp[-Kt^n] \tag{1}$$

The existence of the incubation period and the Avrami exponent values of about 4 indicate that the studied alloy undergoes nucleation and growth-type transformation by polymorphous reaction on heating above the heating-rate dependent crystallization temperature.

Laser beam welding of glassy samples.

XRD patterns of the samples laser-beam welded at different speed are shown in Fig. 3. As well as in the heat treated sample the hR14 Ni₄Ti₃-type phase was found to precipitate within the central area of the sample laser beam welded at 2 and 2.5 m/min (see Figs. 2 and 3). One can see that the volume fraction of the crystalline phase decreases with an increase in the welding speed. The appearance of the welded sample is shown in Fig. 4.

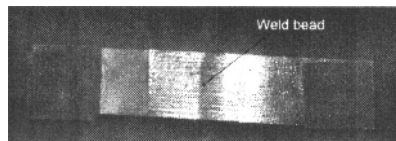


Figure 4. Optical micrograph of the sample subjected for laser beam welding.

The TEM images of the welded zone in the sample welded at 2.5 m/min arc shown in Fig. 5. The existence of the submicron hR14 Ni_4Ti_3 solid solution type particles is observed in some parts of the sample (Fig. 5 (a)). Fig. 5 (b,c) shows the selected-area electron diffraction (SAED) patterns indexed according to hR14 lattice. The chemical composition of these multicomponent crystalline particles and a residual amorphous phase after welding arc shown in Table 1.

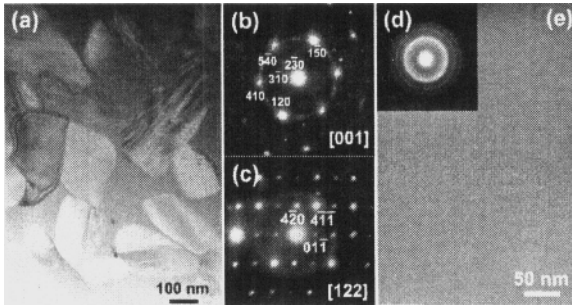


Figure 5. TEM images of the studied alloy. (a) welded zone and (e) the area around the welded zone (heat affected zone). (b and c) SAED patterns taken from the crystalline particles in (a) and indexed according to hR14 Ni_4Ti_3 phase lattice. (d) SAED from the area in (e).

Table 1. Chemical composition of the hR14 crystalline particles and a residual amorphous phase after welding (at%).

	Ni	Nb	Ti	Zr	Co	Cu
Crystal 1	47.6	29.3	10.2	5.2	4.8	2.9
Crystal 2	46.2	30.1	6.0	10.3	4.7	2.8
Amorph.	45.5	30.9	6.9	9.0	4.8	3.0

The areas around the welded zone with a large volume fraction of the glassy phase (Fig. 5 (e)) contain nanocrystals of Ni_4Ti_3 . The laser beam welded sample showed a tensile mechanical strength of 410 MPa.

Electron-beam welding of glassy samples.

The electron-beam welded samples shown in Fig. 6 were found to be almost amorphous (Fig. 7). In other words the volume fraction of crystalline particles is lower compared to those in the laser-beam welded samples. A low fraction of the crystalline particles were found in the welded zone of the sample electron-beam welded at the welding current of 4 mA. However, in some places the surface of the welded sample was oxidized. According to XRD data no crystals were found in the thermally affected area around the welded zone.

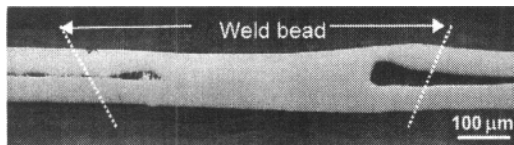


Figure 6. The edge of the welded bead in the sample welded by electron-beam at a beam current of 3.9 mA.

SEM.

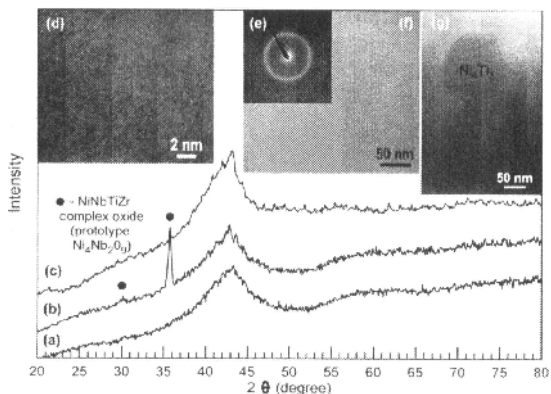


Figure 7. (a-c) XRD patterns and (d-g) TEM images of the electron-welded sample of the studied alloy. XRD of the welded zone: (a) clear area and (b) oxidized area and (c) thermally affected area. (d) HRTEM image inside the welded zone. (e) SAED pattern. (f) bright-field image of the amorphous area. (g) a single particle of the hR14 Ni_4Ti_3 phase.

The electron beam welded samples showed much higher tensile strength (960 MPa) compared to the laser beam welded samples. No oxide particles were found in the body of the sample, which allows us to conclude that the oxidation took place on the surface only.

DISCUSSION

The studied glassy alloy exhibits a large supercooled liquid region on heating and initially crystallizes by polymorphous reaction using nucleation and growth mechanism forming uniaxial grains of a metastable hR14 Ni_4Ti_3 solid solution phase (LM Co and Cu may substitute Ni while ELM Zr and Nb are presumed to substitute Ti). The kinetic analysis confirmed the interface-controlled polymorphous transformation mechanism observed. An Avrami exponent value of about 4 suggests the interface-controlled growth. The lattice parameters of the multicomponent hR14 Ni_4Ti_3 phase are slightly different from those¹⁶ of a binary phase, hR14 $\text{Ni}_{4.5}\text{Nb}_{6.5}$ phase and an unidentified phase form at higher temperature while the hR14 Ni_4Ti_3 phase disappears.

Successful bonding is achieved after both laser-beam and electron beam welding. Electron-beam welding produces somewhat better results compared to laser beam one. Almost fully amorphous samples were obtained with a small volume fraction of the hR14 Ni_4Ti_3 solid solution crystalline phase upon electron-beam welding, though some surface oxidation was observed due to insufficient vacuum. A complex oxide formed in some parts of the surface has a structure of $\text{Ni}_4\text{Nb}_2\text{O}_9$ one. The obtained results indicate high stability of the sample upon heating. It is also found that with an increase in the laser-beam welding speed from 2 to 3 m/min the structure of the welded zone changes from the amorphous + hR14 Ni_4Ti_3 crystalline phase to an almost single amorphous one. By adjusting the welding speed one can obtain the desired microstructure. Within the sample welded at 2.5 m/min the metastable Ni_4Ti_3 particle size varied from a few nanometres in the outer area of the welded zone to a few hundreds of nanometres in the center. The electron-beam samples welded at the beam current of 4 mA, voltage of 60 kV and a speed of 4 m/min were found to be almost amorphous.

The crystallization behavior and the structure of the welded samples of the $\text{Ni}_{53}\text{Nb}_{20}\text{Ti}_{10}\text{Zr}_8\text{Co}_6\text{Cu}_3$ alloy were studied. The results indicate successful welding of the glassy alloy by the electron-beam welding. The obtained data are promising for future applications of the laser and electron-beam welding techniques to glassy alloys.

REFERENCES:

- ¹ A. Inoue, "High-strength bulk amorphous alloys with low critical cooling rates" *Mater. Trans. JIM* 36, 866-875 (1995).
- ² A. Inoue, "Stabilization of metallic supercooled liquid and bulk amorphous alloys" *Acta Mater.* 48, 279-306 (2000).
- ³ W. L. Johnson, "Bulk glass forming metallic alloys: science and technology" *MRS Bull* 24, 42-56 (1999).
- ⁴ S. Yi, T.G. Park and D.H. Kim, "Ni-based bulk amorphous alloys in the Ni-Ti-Zr-(Si, Sn) system" *J. Mater. Res.* 15, 2425-2429 (2000).
- ⁵ J.K. Lee, S.H. Kim, S. Yi, W.T. Kim and D.H. Kim, "A Study on the Development of Ni-Based Alloys with Wide Supercooled Liquid Region" *Mater. Trans. JIM* 42, 592-596 (2001).
- ⁶ A. Inoue, W. Zhang and T. Zhang, "Thermal Stability and Mechanical Strength of Bulk Glassy Ni-Nb-Ti-Zr Alloys" *Mater. Trans.* 43, 1952-1956 (2002).
- ⁷ W. Zhang and A. Inoue, "Effects of Ti on the Thermal Stability and Glass-Forming Ability of Ni-Nb Glassy Alloy" *Mater. Trans.* 43, 2342-2345 (2002).
- ⁸ T. C. Hufnagel, C. Fan, R. T. Ott, J. Li, S. Brennan, "Controlling shear band behavior in metallic glasses through microstructural design" *Intermetallics* 10, 1163-1168 (2002).
- ⁹ W. Zhang, A. Inoue, "Formation and Mechanical Properties of Ni-based Ni-Nb-Ti-Hf Bulk Glassy Alloys" *Scripta Mater.* 48, 641-645 (2003).
- ¹⁰ H. Choi-Yim, D. Xu, and W. L. Johnson, "Ni-based Bulk Metallic Glass Formation in the Ni-Nb-Sn and Ni-Nb-Sn-X (X=B,Fe,Cu) Alloy System" *Appl. Phys. Lett.* 82, 1030-1032 (2003).
- ¹¹ T. Zhang and A. Inoue, "New Bulk Glassy Ni-Based Alloys with High Strength of 3000 MPa" *Mater. Trans. JIM* 43, 708-711 (2002).
- ¹² M.H. Lee, J.Y. Lee, D.H. Bae, W.T. Kim, D.J. Sordelet, D.H. Kim, "A development of Ni-based alloys with enhanced plasticity" *Intermetallics* 12, 1133-1137 (2004).
- ¹³ T. Shimada, D. V. Louzguine, J. Saida and A. Inoue "Thermal Stability and Devitrification Behavior of Ternary Ni-Nb-Ti and Quaternary Glassy Alloys Containing Noble Metals" *Materials Transactions*, 46, 675-680 (2005).
- ¹⁴ D. V. Louzguine-Luzgin, T. Shimada and A. Inoue "Ni-based bulk glassy alloys with large supercooled liquid region exceeding 90 K" *Intermetallics*, 13, 1166-1171 (2005)
- ¹⁵ J.W. Christian "The Theory of Transformation in Metals and Alloys" Oxford: Pergamon Press Ltd; 1975. p. 542.
- ¹⁶ T. Saburi, T. Tatsumi and S. Nenno "Effects of heat treatment on mechanical behavior of Ti-Ni alloys" *Journal de Physique C4*, 261-266 (1982).